

Roton entanglement in quenched dipolar Bose-Einstein condensates

Zehua Tian, Seok-Yeong Chä, and Uwe R. Fischer
*Seoul National University, Department of Physics and Astronomy,
 Center for Theoretical Physics, Seoul 08826, Korea*

We study quasi-two-dimensional dipolar Bose-Einstein condensates, in which the Bogoliubov excitation spectrum displays, at sufficiently large gas density, a deep roton minimum due to the spatially anisotropic behavior of the dipolar two-body potential. A rapid quench, performed on the speed of sound of excitations propagating on the condensate background, leads to the dynamical Casimir effect, which can be characterized by measuring the density-density correlation function. It is shown, for both zero and finite initial temperatures, that the continuous-variable bipartite quantum state of the created quasiparticle pairs with opposite momenta, resulting from the quench, displays an enhanced potential for the presence of entanglement (represented by nonseparable and steerable quasiparticle states), when compared to a gas with solely repulsive contact interactions. Steerable quasiparticle pairs contain momenta from close to the roton, and hence quantum correlations significantly increase in the presence of a deep roton minimum.

I. INTRODUCTION

Quantum field theory predicts that pairs of correlated particles are created from the vacuum when the classical background rapidly varies in time [1]. This process can take place in the expanding (or contracting) universe, where it is coined cosmological particle production [2, 3], and occurs analogously in the dynamical Casimir effect for photons generated from the electro-dynamical quantum vacuum in a vibrating cavity [4]. Correlated pairs of particles are also created by the phenomenon of Hawking radiation in the presence of an event horizon [5, 6].

The pairs produced by temporal variations of a homogeneous background consist of quanta with opposite momenta and form (continuous-variable) bipartite quantum states. Directly observing pair creation in relativistic quantum field theory is notoriously difficult due to the challenging experimental requirements for achieving sizable pair production rates. To render pair creation, under rather general conditions, accessible to experiment, the idea of quantum simulation [7] was applied to relativistic quantum fields on effective curved spacetime [8, 9]. This is frequently classified under the notion of “analogue gravity,” see Ref. [10] for an extensive review and a comprehensive list of references. Several quantum simulation experiments, in which quasiparticles propagate on a rapidly changing background, leading to the dynamical Casimir effect (or analogue cosmological particle production when the induced spacetime metric has a cosmological form), have been proposed, e.g., in [11–16] and experiments have been conducted, cf., e.g., [17–20]. In the same vein, to investigate analogue event and cosmological horizons and the associated effects, several experiments have been proposed [21–27] and some were realized in the lab [28–32].

We study in what follows the quantum field theoretical

phenomenon of pair creation in a quasi-two-dimensional (quasi-2D) Bose-Einstein condensate (BEC) with dipolar interactions. Subjecting the dipolar BEC to rapid temporal changes (quenches) of the condensate background, we investigate the production of pairs of quasiparticles and their quantum correlations. To assess, then, whether nonseparability and steerability of quasiparticle excitations are present, we employ the density-density correlations created by the quench [27, 33].

Magnetic dipole-dipole interaction (DDI) dominated condensates [34] have been realized with chromium [35], dysprosium [36], and erbium [37] atoms, and the realization of BECs made up of molecules with permanent electric dipoles [38] is now at the forefront of ongoing research cf., e.g., [39, 40]. For the creation of quasiparticle pairs in a time-dependent background, we will demonstrate that the existence of a deep *roton minimum* in the excitation spectrum [41–45] plays a dominant role. Various ramifications of the dipolar BEC roton, originally defined for and observed in the strongly interacting superfluid helium II [46, 47], have been recently experimentally investigated in ultracold dipolar quantum gases [48–51]. We will argue below that quantum correlations, here represented by the nonseparability and steerability present in a bipartite continuous variable system, are significantly enhanced in the presence of a deep roton minimum, that is, for sufficiently large densities of a DDI dominated gas.

In quantum simulation–analogue gravity language, we study the quasiparticle production due to the dynamical Casimir effect for a (in the low-momentum corner) relativistic quantum field (the phonon). In the ultracold quantum gas, the shape of the (analogue) Planckian, Lorentz-invariance-breaking, large-momentum sector of the spectrum around the roton minimum is well controlled. We exploit in what follows that the analogue Planckian sector can be *engineered*, to explore the

consequences for the quantum many-body state of the quasiparticles created by a quench.

II. PAIR CREATION OF QUASIPARTICLES IN A QUASI-2D DIPOLAR GAS

A. Scaling transformation

We consider an interacting Bose gas comprising atoms or molecules with mass m . Its Lagrangian density is given by ($\hbar = 1$)

$$\mathcal{L} = \frac{i}{2}(\Psi^* \partial_t \Psi - \partial_t \Psi^* \Psi) - \frac{1}{2m} |\nabla \Psi|^2 - V_{\text{ext}} |\Psi|^2 - \frac{1}{2} |\Psi|^2 \int d^3 \mathbf{R}' V_{\text{int}}(\mathbf{R} - \mathbf{R}') |\Psi(\mathbf{R}')|^2. \quad (1)$$

In the above, $\mathbf{R} = (\mathbf{r}, z)$ are spatial 3D coordinates. The system is trapped by an external potential of the form $V_{\text{ext}}(\mathbf{R}, t) = m\omega^2 \mathbf{r}^2/2 + m\omega_z^2 z^2/2$, where both ω and ω_z can in general be time-dependent. We will assume that over the whole time evolution, the gas is strongly confined in z direction, with aspect ratio $\kappa = \omega_z/\omega \gg 1$. We also assume quasi-homogeneity in the plane, i.e. that the relevant wavelengths of quasiparticle excitations are much shorter than the inhomogeneity scale caused by the in-plane harmonic trapping.

The two-body interaction is given by

$$V_{\text{int}}(\mathbf{R} - \mathbf{R}') = g_c \delta^3(\mathbf{R} - \mathbf{R}') + V_{\text{dd}}(\mathbf{R} - \mathbf{R}'), \quad (2)$$

where g_c is the contact interaction coupling, and $V_{\text{dd}}(\mathbf{R} - \mathbf{R}') = 3g_d[(1 - 3(z - z')^2/|\mathbf{R} - \mathbf{R}'|^2)/|\mathbf{R} - \mathbf{R}'|^3]/4\pi$ describes the dipolar interaction with coupling constant g_d . The dipoles are assumed to be polarized along the z -direction by an external field. In general, g_c and g_d can be time-dependent, depending on the protocol of condensate expansion or contraction which is implemented, see below. We denote by $g_{c,0}$ and $g_{d,0}$ their initial, $t = 0$, values.

To ensure stability in the DDI dominated regime [42], we impose that the system remains in the quasi-2D regime during its whole temporal evolution. In z direction, we thus assume that the condensate density is a Gaussian, $\rho_z(z) = (\pi d_z^2)^{-1/2} \exp[-z^2/d_z^2]$, where $d_z = b(t)d_{z,0}$ with $d_{z,0} = 1/\sqrt{m\omega_{z,0}}$ and $b(t)$ the scale factor [45]. We can then integrate out the z dependence and obtain the effective quasi-2D interaction, which is given by $V_{\text{int}}^{2D}(\mathbf{r} - \mathbf{r}') = \int dz dz' V_{\text{int}}(\mathbf{R} - \mathbf{R}') \rho_z(z) \rho_z(z')$.

Under the usual scaling transformation [52, 53], laid down in a very general form in [54], which is applicable to BECs with both time-dependent trapping and coupling constants, one imposes that the *scaling variables* \mathbf{x} , τ ,

and ψ obey

$$\mathbf{x} = \frac{\mathbf{r}}{b(t)}, \quad \tau = \int_0^t \frac{dt'}{b^2(t')},$$

$$\Psi(\mathbf{r}, t) = \exp \left[i \frac{mr^2}{2} \frac{\partial_t b}{b} \right] \frac{\psi(\mathbf{x}, \tau)}{b}. \quad (3)$$

We introduce a factor $f^2 = f^2(t)$ in the following, also see the Heisenberg Eq. (5) below. It encapsulates the effects of time-dependent trapping frequency and coupling in the following equation of motion for the scale factor b [45, 54]

$$\frac{b^3 \partial_t^2 b + b^4 \omega^2(t)}{\omega_0^2} = \frac{g_c(t)}{g_{c,0}b} = \frac{g_d(t)}{g_{d,0}b} =: f^2(t). \quad (4)$$

Given experimentally prescribed time dependences of trapping and couplings, the above relation determines the scaling expansion. On the other hand, given a desired scaling expansion or contraction $b = b(t)$, to which, e.g., the speed of sound $c = c(t)$ time dependence is related by Eq. (19) below via $f(t)$, one can determine the required trapping frequencies, imposing possibly in addition a temporal dependence of the coupling constants. Note that for the scaling approach to accurately yield the expansion or contraction dependence of the field operator in a gas with both contact and dipolar interactions present (i.e., for the scaling evolution to follow a symmetry), the contact (g_c) and dipole (g_d) couplings are required to either have an identical time dependence, or to both remain constant. We remark that when one of the $g_{c,0}$, $g_{d,0}$ equals zero, the terms $g_c(t)/g_{c,0}b$ or $g_d(t)/g_{d,0}b$, respectively, do not appear as a constraint in the equation (4) for f^2 .

With the above definitions, the Heisenberg equation of motion for the scaling field operator $\hat{\psi}(\mathbf{x}, \tau)$ reads

$$i\partial_\tau \hat{\psi} = \left[-\frac{1}{2m} \nabla_{\mathbf{x}}^2 + f^2 \frac{m}{2} \omega_0^2 \mathbf{x}^2 + f^2 \int d^2 \mathbf{x}' V_{\text{int},0}^{2D}(\mathbf{x} - \mathbf{x}') \hat{\psi}^\dagger(\mathbf{x}') \hat{\psi}(\mathbf{x}') \right] \hat{\psi}. \quad (5)$$

with $\omega_0 = \omega(t=0)$ the initial trapping frequency.

The quasi-2D dipole-dipole scaling interaction is Fourier transformed according to $V_{\text{int},0}^{2D}(\mathbf{k}) = \int d^2 \mathbf{x} e^{-i\mathbf{k} \cdot \mathbf{x}} V_{\text{int},0}^{2D}(\mathbf{x})$. We set the (initial) normalization area of the plane to unity in the definition of Fourier transforms and their inverse. Also, here and in what follows \mathbf{k} represents *comoving (scaling) momentum*, as we work in the scaling frame of reference. The Fourier transform of the interaction is obtained to be [42]

$$V_{\text{int},0}^{2D}(k) = g_0^{\text{eff}} \left(1 - \frac{3R}{2} \zeta w \left[\frac{\zeta}{\sqrt{2}} \right] \right), \quad (6)$$

where $w[z] = \exp[z^2](1 - \operatorname{erf}[z])$ denotes the w function and $\zeta = kd_{z,0}$ is a dimensionless wavenumber. Here, we defined an effective contact coupling

$$g_0^{\text{eff}} = \frac{1}{\sqrt{2\pi}d_{z,0}}(g_{c,0} + 2g_{d,0}) \quad (7)$$

and the dimensionless ratio

$$R = \frac{\sqrt{\pi/2}}{1 + g_{c,0}/2g_{d,0}}. \quad (8)$$

The parameter R ranges from $R = 0$ if $g_{d,0}/g_{c,0} \rightarrow 0$, to $R = \sqrt{\pi/2}$ for $g_{d,0}/g_{c,0} \rightarrow \infty$ and expresses the relative strength of contact and dipolar interactions. In the remainder of the paper, we put either $R = 0$ (contact dominance) or $R = \sqrt{\pi/2}$ (DDI dominance).

B. Bogoliubov-de Gennes equation

We decompose the field operator as follows,

$$\hat{\psi} = \psi_0(1 + \hat{\phi}),$$

where $|\psi_0(\mathbf{x}, \tau)|^2 = \rho_0$ represents the condensate density, and where $\hat{\phi}$ describes the perturbations (excitations) on top of the condensate. The Bogoliubov-de Gennes equation obeyed by the fluctuation field $\hat{\phi}$ reads [55]

$$i\partial_\tau \hat{\phi} = \mathcal{H}\hat{\phi} + \mathcal{A}(\hat{\phi} + \hat{\phi}^\dagger), \quad (9)$$

in which we define two operators \mathcal{H} , \mathcal{A} by

$$\mathcal{H} = -\frac{1}{2m}\nabla_{\mathbf{x}}^2 - \frac{1}{m\sqrt{\rho_0}}(\nabla_{\mathbf{x}}\sqrt{\rho_0}) \cdot \nabla_{\mathbf{x}} - i\mathbf{v}_{\text{com}} \cdot \nabla_{\mathbf{x}}, \quad (10)$$

$$\mathcal{A}F = f^2 \int d^2\mathbf{x}' V_{\text{int},0}^{2D}(\mathbf{x} - \mathbf{x}')|\psi_0(\mathbf{x}')|^2 F(\mathbf{x}').$$

where \mathcal{A} acts by convolution on an arbitrary function $F(\mathbf{x})$. Here $\mathbf{v}_{\text{com}} = \frac{1}{m}\nabla_{\mathbf{x}}\theta_0$, where $\psi_0 = \sqrt{\rho_0}e^{i\theta_0}$, denotes the comoving frame velocity [45].

Assuming vanishingly small comoving velocity, $\mathbf{v}_{\text{com}} = 0$, and quasi-homogeneity, $\nabla_{\mathbf{x}}\sqrt{\rho_0} \simeq \mathbf{0}$, then ρ_0 and θ_0 become independent of \mathbf{x} , and we obtain

$$i\partial_\tau \hat{\phi} = -\frac{1}{2m}\nabla_{\mathbf{x}}^2 \hat{\phi} + f^2 \rho_0 \int d^2\mathbf{x}' V_{\text{int},0}^{2D}(\mathbf{x} - \mathbf{x}')(\hat{\phi}(\mathbf{x}') + \hat{\phi}^\dagger(\mathbf{x}')). \quad (11)$$

In momentum space, we decompose the fluctuations into their Fourier components, $\hat{\phi}(\mathbf{x}) = (1/\sqrt{N})\sum_{\mathbf{k}} e^{i\mathbf{k}\cdot\mathbf{x}}\hat{\phi}_{\mathbf{k}}$, $\hat{\phi}_{\mathbf{k}} = \sqrt{N}\int d^2\mathbf{x} e^{-i\mathbf{k}\cdot\mathbf{x}}\hat{\phi}(\mathbf{x})$ with N being the total number of atoms in the condensate.

We then have the Fourier space Bogoliubov-de Gennes equation

$$i\partial_\tau \begin{bmatrix} \hat{\phi}_{\mathbf{k}} \\ \hat{\phi}_{-\mathbf{k}}^\dagger \end{bmatrix} = \begin{bmatrix} \mathcal{H}_{\mathbf{k}} + \mathcal{A}_{\mathbf{k}} & \mathcal{A}_{\mathbf{k}} \\ -\mathcal{A}_{\mathbf{k}} & -(\mathcal{H}_{\mathbf{k}} + \mathcal{A}_{\mathbf{k}}) \end{bmatrix} \begin{bmatrix} \hat{\phi}_{\mathbf{k}} \\ \hat{\phi}_{-\mathbf{k}}^\dagger \end{bmatrix}. \quad (12)$$

Here, single-particle and interaction energy terms respectively read

$$\mathcal{H}_{\mathbf{k}} = \frac{k^2}{2m}, \quad \mathcal{A}_{\mathbf{k}} = f^2 \rho_0 V_{\text{int},0}^{2D}(k). \quad (13)$$

To diagonalize (12), we thus apply a Bogoliubov transformation with coefficients $u_{\mathbf{k}}$ and $v_{\mathbf{k}}$ as follows:

$$\begin{bmatrix} \hat{\phi}_{\mathbf{k}} \\ \hat{\phi}_{-\mathbf{k}}^\dagger \end{bmatrix} = \begin{bmatrix} u_{\mathbf{k}} & v_{\mathbf{k}} \\ v_{\mathbf{k}} & u_{\mathbf{k}} \end{bmatrix} \begin{bmatrix} \hat{\varphi}_{\mathbf{k}} \\ \hat{\varphi}_{-\mathbf{k}}^\dagger \end{bmatrix}, \quad (14)$$

where $\hat{\phi}_{\mathbf{k}}$ and $\hat{\varphi}_{\mathbf{k}}$ respectively represent the original fluctuation operators and the Bogoliubov quasiparticle operators. Also note that the bosonic algebra imposes

$$u_{\mathbf{k}}^2 - v_{\mathbf{k}}^2 = 1. \quad (15)$$

Thereby solving the eigenproblem of (12), we obtain

$$\begin{bmatrix} u_{\mathbf{k}} \\ v_{\mathbf{k}} \end{bmatrix} = \frac{\sqrt{\mathcal{H}_{\mathbf{k}}} \pm \sqrt{\mathcal{H}_{\mathbf{k}} + 2\mathcal{A}_{\mathbf{k}}}}{2(\mathcal{H}_{\mathbf{k}}^2 + 2\mathcal{H}_{\mathbf{k}}\mathcal{A}_{\mathbf{k}})^{1/4}}, \quad (16)$$

where where the upper and lower signs refer to $u_{\mathbf{k}}$ and $v_{\mathbf{k}}$, respectively. Then, $[u_{\mathbf{k}} \ v_{\mathbf{k}}]^T$ is the eigenvector with eigenvalue $\sqrt{\mathcal{H}_{\mathbf{k}}^2 + 2\mathcal{H}_{\mathbf{k}}\mathcal{A}_{\mathbf{k}}}$, and $[v_{\mathbf{k}} \ u_{\mathbf{k}}]^T$ is the eigenvector with eigenvalue $-\sqrt{\mathcal{H}_{\mathbf{k}}^2 + 2\mathcal{H}_{\mathbf{k}}\mathcal{A}_{\mathbf{k}}}$.

In general, the excitation frequencies are scaling time dependent, and Eq. (12) yields

$$i\partial_\tau \begin{bmatrix} \hat{\varphi}_{\mathbf{k}} \\ \hat{\varphi}_{-\mathbf{k}}^\dagger \end{bmatrix} = \begin{bmatrix} \omega_{\mathbf{k}} & +i\partial_\tau \omega_{\mathbf{k}}/2\omega_{\mathbf{k}} \\ +i\partial_\tau \omega_{\mathbf{k}}/2\omega_{\mathbf{k}} & -\omega_{\mathbf{k}} \end{bmatrix} \begin{bmatrix} \hat{\varphi}_{\mathbf{k}} \\ \hat{\varphi}_{-\mathbf{k}}^\dagger \end{bmatrix}, \quad (17)$$

where the excitation spectrum is given by

$$\omega_{\mathbf{k}}(\tau) = \sqrt{\mathcal{H}_{\mathbf{k}}^2 + 2\mathcal{H}_{\mathbf{k}}\mathcal{A}_{\mathbf{k}}(\tau)}. \quad (18)$$

Here, we introduce the parameter,

$$c(\tau) = f(\tau)\sqrt{g_0^{\text{eff}}\rho_0/m} = f(\tau)c_0, \quad (19)$$

which is the (scaling time dependent) speed of sound. It is the slope of the linear, low- \mathbf{k} part of the dispersion relation (18). We may also define, in addition to R in (8), another dimensionless parameter

$$A = \frac{mc_0^2}{\omega_{z,0}} = \frac{g_0^{\text{eff}}\rho_0}{\omega_{z,0}}, \quad (20)$$

representing an effective chemical potential as measured relative to the (initial) transverse trapping, linear in both

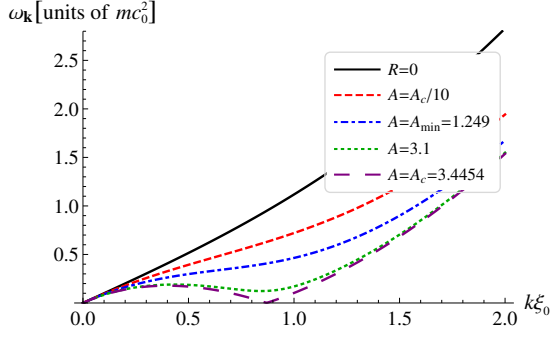


FIG. 1. (Color online) *Stationary state excitation spectrum.* Bogoliubov excitation energy in units of mc_0^2 , for DDI dominance, $R = \sqrt{\pi}/2$. For $A > A_{\min} = 1.249$, the spectrum develops a roton minimum and becomes unstable for $A > A_c = 3.4454$. $R = 0$ denotes the contact interaction case where the Bogoliubov excitation energy, when normalized to mc_0^2 , as here, is independent of A ; ξ_0 is the healing length defined in (II B).

the condensate density and the effective contact coupling defined in (7).

For a stationary state $f = 1$ [$c(\tau) = c_0$], the healing length is given by

$$\xi_0 = \frac{1}{mc_0}. \quad (21)$$

The inverse of ξ_0 , $k_{P1} := 1/\xi_0$, is an analogue “Planck scale.” Close to the roton minimum at $k\xi_0 \approx 0.9$, then, Lorentz invariance is strongly broken and a particular variant of *Planckian* ($k \sim k_{P1}$) physics can be simulated [45]. In Fig. 1, we plot the corresponding stationary state Bogoliubov excitation energy, from which we see that the spectrum in a strongly dipolar BEC develops a roton minimum for sufficiently large A . The system becomes unstable past the critical value $A = A_c = 3.4454$ (when $R = \sqrt{\pi}/2$ [42]). In the low-momentum corner, the spectrum is generally linear in momentum,

$$\omega_{\mathbf{k}} = c_0 k \quad (k\xi_0 \ll 1), \quad (22)$$

implying the (pseudo-)Lorentz invariance of the system from which the effective metric concept for the propagating quantum field of phonons emerges [10].

For a stationary system, we find that the operators $\hat{\varphi}_{\mathbf{k}}$ and $\hat{\varphi}_{-\mathbf{k}}^\dagger$ decouple, and oscillate at constant frequencies $\pm\omega_{\mathbf{k}}$, where $\tau = t$ for the stationary case with $f = b = 1$ in (3),

$$\hat{\varphi}_{\mathbf{k}}(\tau) = \hat{b}_{\mathbf{k}} e^{-i\omega_{\mathbf{k}}\tau}, \quad \hat{\varphi}_{-\mathbf{k}}^\dagger(\tau) = \hat{b}_{-\mathbf{k}}^\dagger e^{i\omega_{\mathbf{k}}\tau}. \quad (23)$$

Here $\hat{b}_{\mathbf{k}}$ and $\hat{b}_{\mathbf{k}}^\dagger$ are, respectively, annihilation and creation operators of collective excitations with momentum \mathbf{k} above the stationary condensate.

C. Mode mixing

As a result of a rapid temporal change of c^2 , as defined in (19), and which is encoded in the scale factor f defined in (4), Eq. (17) engenders mode mixing between the quasiparticle modes of momenta \mathbf{k} and $-\mathbf{k}$, which entails the amplification of quantum and thermal fluctuations. It is convenient to characterize the mode mixing by introducing the coefficients $\alpha_{\mathbf{k}}(\tau)$ and $\beta_{\mathbf{k}}(\tau)$ [56]:

$$\begin{aligned} \hat{\varphi}_{\mathbf{k}}(\tau) &= \left[\alpha_{\mathbf{k}}(\tau) \hat{b}_{\mathbf{k}}^{\text{in}} + \beta_{\mathbf{k}}^*(\tau) \hat{b}_{-\mathbf{k}}^{\text{in}\dagger} \right] \exp \left[-i \int^\tau \omega_{\mathbf{k}}(\tau') d\tau' \right], \\ \hat{\varphi}_{-\mathbf{k}}^\dagger(\tau) &= \left[\alpha_{\mathbf{k}}^*(\tau) \hat{b}_{-\mathbf{k}}^{\text{in}\dagger} + \beta_{\mathbf{k}}(\tau) \hat{b}_{\mathbf{k}}^{\text{in}} \right] \exp \left[i \int^\tau \omega_{\mathbf{k}}(\tau') d\tau' \right]. \end{aligned} \quad (24)$$

In the limit $\tau \rightarrow -\infty$, $\hat{b}_{\mathbf{k}}^{\text{in}}$ and $\hat{b}_{-\mathbf{k}}^{\text{in}\dagger}$ are defined such that $\hat{\varphi}_{\mathbf{k}}(\tau) \rightarrow \hat{b}_{\mathbf{k}}^{\text{in}} e^{-i\omega_{\mathbf{k}}\tau}$, $\hat{\varphi}_{-\mathbf{k}}^\dagger(\tau) \rightarrow \hat{b}_{-\mathbf{k}}^{\text{in}\dagger} e^{i\omega_{\mathbf{k}}\tau}$, or equivalently, $\alpha_{\mathbf{k}} \rightarrow 1$ and $\beta_{\mathbf{k}} \rightarrow 0$ as $\tau \rightarrow -\infty$. That is to say, the operators $\hat{b}_{\mathbf{k}}^{\text{in}}$ and $\hat{b}_{-\mathbf{k}}^{\text{in}\dagger}$ are, respectively, the annihilation and creation operators of collective excitations with momentum \mathbf{k} in the initial stationary state. From Eqs. (17) and (24), we find that the evolution of the operators $\hat{\varphi}_{\mathbf{k}}(\tau)$ and $\hat{\varphi}_{-\mathbf{k}}^\dagger(\tau)$ is completely determined by $\alpha_{\mathbf{k}}(\tau)$ and $\beta_{\mathbf{k}}(\tau)$, and the corresponding evolution equations of $\alpha_{\mathbf{k}}(\tau)$ and $\beta_{\mathbf{k}}(\tau)$ are:

$$\begin{aligned} \partial_\tau \alpha_{\mathbf{k}} &= + \frac{\partial_\tau \omega_{\mathbf{k}}}{2\omega_{\mathbf{k}}} \exp \left(2i \int^\tau \omega_{\mathbf{k}}(\tau') d\tau' \right) \beta_{\mathbf{k}}, \\ \partial_\tau \beta_{\mathbf{k}} &= + \frac{\partial_\tau \omega_{\mathbf{k}}}{2\omega_{\mathbf{k}}} \exp \left(-2i \int^\tau \omega_{\mathbf{k}}(\tau') d\tau' \right) \alpha_{\mathbf{k}}. \end{aligned} \quad (25)$$

Given the temporal change $c^2 = c^2(\tau)$, the above equations can be solved to obtain $\alpha_{\mathbf{k}}(\tau)$ and $\beta_{\mathbf{k}}(\tau)$, and hence $\hat{\varphi}_{\mathbf{k}}(\tau)$ and $\hat{\varphi}_{-\mathbf{k}}^\dagger(\tau)$.

The phase factors of $\alpha_{\mathbf{k}}$ and $\beta_{\mathbf{k}}$ in (25) determine the phase of the oscillations of the density-density correlation function (i.e., Eq. (37)) around its mean value. We note in this regard that a typo has occurred in Eqs. (21) and (26) of Ref. [14], where the sign “−” should be a “+”. However, this sign has no effect on the minimal values of the density-density correlation amplitude, which is characterizing the degree of entanglement present in the quasiparticle state after the quench. We shall now turn to the corresponding discussion.

III. CHARACTERIZING NONSEPARABILITY AND STEERABILITY

After a series of identical experiments to measure the density distribution of the gas, we can extract its mean, as well as the fluctuations around this mean. The corresponding density-density correlations [57] are related to the quasiparticle quantum state [33]. We will proceed

to demonstrate how to use these correlations to measure nonseparability and steerability between the created quasiparticles with opposite momenta \mathbf{k} and $-\mathbf{k}$, which are due to temporal variations of the condensate background. Below, we closely follow the density-density correlation-function based discussion of the criteria for nonseparability and steerability previously laid down in Refs. [14, 27].

A. The density-density correlation function

The total atom number density in the condensate is given to linear order in the fluctuations by

$$\hat{\rho}(\tau, \mathbf{x}) = \hat{\psi}^\dagger(\tau, \mathbf{x})\hat{\psi}(\tau, \mathbf{x}) \simeq \rho_0(1 + \hat{\phi}^\dagger(\tau, \mathbf{x}) + \hat{\phi}(\tau, \mathbf{x})). \quad (26)$$

In a homogeneous system, the background density ρ_0 is constant, and the relative density fluctuation is

$$\frac{\delta\hat{\rho}(\tau, \mathbf{x})}{\rho_0} = \frac{\hat{\rho}(\tau, \mathbf{x}) - \rho_0}{\rho_0} = \hat{\phi}^\dagger(\tau, \mathbf{x}) + \hat{\phi}(\tau, \mathbf{x}). \quad (27)$$

We consider *in situ* measurements of $\delta\hat{\rho}(\tau, \mathbf{x})$ performed at some (scaling) measurement time $\tau = \tau_m$. From the equal-time commutators $[\hat{\psi}(\tau, \mathbf{x}), \hat{\psi}(\tau, \mathbf{x}')] = 0$ and $[\hat{\psi}(\tau, \mathbf{x}), \hat{\psi}^\dagger(\tau, \mathbf{x}')] = \delta(\mathbf{x} - \mathbf{x}')$, one can easily verify that $\delta\hat{\rho}(\tau, \mathbf{x})$ and $\delta\hat{\rho}(\tau, \mathbf{x}')$ commute with each other.

In momentum space, we express the relative density fluctuation (27) in terms of quasiparticle operators,

$$\begin{aligned} \frac{\delta\hat{\rho}_{\mathbf{k}}(\tau)}{\rho_0} &= \hat{\phi}_{\mathbf{k}}(\tau) + \hat{\phi}_{-\mathbf{k}}^\dagger(\tau) \\ &= (u_{\mathbf{k}} + v_{\mathbf{k}})(\hat{\varphi}_{\mathbf{k}}(\tau) + \hat{\varphi}_{-\mathbf{k}}^\dagger(\tau)). \end{aligned} \quad (28)$$

Note that taking the Hermitian conjugate of the operator (28) is equivalent to changing the sign of \mathbf{k} , as a consequence of the fact that the relative density fluctuation operator in (27) is itself a Hermitian operator and thus is an observable (the results of the corresponding measurement are real quantities). It is straightforward to show that this operator commutes with its Hermitian conjugate, and thus the following correlation function is well defined:

$$\begin{aligned} G_{2,\mathbf{k}}(\tau) &= \frac{\langle |\delta\hat{\rho}_{\mathbf{k}}(\tau)|^2 \rangle}{\rho_0^2} \\ &= (u_{\mathbf{k}} + v_{\mathbf{k}})^2 (2n_{\mathbf{k}} + 1 + 2\Re[c_{\mathbf{k}} e^{-2i\omega_{\mathbf{k}}\tau}]), \end{aligned} \quad (29)$$

where $n_{\mathbf{k}} = \langle \hat{b}_{\mathbf{k}}^\dagger \hat{b}_{\mathbf{k}} \rangle$ is mean occupation number, and $c_{\mathbf{k}} = \langle \hat{b}_{\mathbf{k}} \hat{b}_{-\mathbf{k}} \rangle$ is pair amplitude. To obtain the above relation, the assumption $n_{\mathbf{k}} = n_{-\mathbf{k}}$ has been made. The second line holds when the background has reached a stationary state, so that the frequencies $\omega_{\mathbf{k}}$ become time-independent.

The mean occupation number $n_{\mathbf{k}}$ determines the time-averaged mean of $G_{2,\mathbf{k}}(\tau)$, while the magnitude and phase of the correlation $c_{\mathbf{k}}$ respectively determine the magnitude and phase of the oscillations of $G_{2,\mathbf{k}}(\tau)$ around its mean value. For the zero temperature (quasiparticle vacuum) case, i.e., $n_{\mathbf{k}} = 0$ (and hence $c_{\mathbf{k}} = 0$), in the correlation function there is just one constant term (the “+1”) left, which is measurable as well and encodes the vacuum fluctuations of the quasiparticle field. This will become of importance later on.

For a thermal initial state with the equilibrium distribution $2n_{\mathbf{k}} + 1 = \coth(\omega_{\mathbf{k}}/2T)$, the term containing $c_{\mathbf{k}}$ vanishes and the correlation function in Eq. (29) reads

$$G_{2,\mathbf{k}} = \frac{k\xi_0/2}{\sqrt{\left(\frac{k\xi_0}{2}\right)^2 + 1 - \frac{3R}{2}k\xi_0\sqrt{Aw}\left[\frac{k\xi_0}{\sqrt{2}}\sqrt{A}\right]}} \coth \left[\frac{k\xi_0\sqrt{\left(\frac{k\xi_0}{2}\right)^2 + 1 - \frac{3R}{2}k\xi_0\sqrt{Aw}\left[\frac{k\xi_0}{\sqrt{2}}\sqrt{A}\right]}}{2T/mc_0^2} \right]. \quad (30)$$

In Fig. 2, we plot the thermal density-density correlation function (30) of a dipolar BEC at various initial temperatures (in units of mc_0^2), and as a function of the nondimensionalized momentum $k\xi_0$, with fixed A and R . We see that the density-density correlation function is strongly modified near the roton minimum of the spectrum. In particular, when the roton minimum approaches zero (near criticality), the modification of the density-density correlation function relative to the pure contact case diverges.

We now discuss the high- and low-temperature limits of (30) separately. When $\omega_{\mathbf{k}}/T \ll 1$, we have $2n_{\mathbf{k}} + 1 = \coth(\omega_{\mathbf{k}}/2T) \simeq 2T/\omega_{\mathbf{k}} + \omega_{\mathbf{k}}/6T$, so that Eq. (30) becomes in the low-momentum (phonon) limit, expanding to quadratic order in $k\xi_0$,

$$\begin{aligned} G_{2,\mathbf{k}} &= \frac{T}{mc_0^2} \left[1 + \frac{3}{2}\sqrt{AR}k\xi_0 \right] \\ &\quad - \left[\frac{T}{mc_0^2} \left(\frac{1}{4} + \frac{3AR}{\sqrt{2\pi}} + \frac{9AR^2}{4} \right) - \frac{mc_0^2}{12T} \right] (k\xi_0)^2 \\ &\quad + \mathcal{O}((k\xi_0)^3). \end{aligned} \quad (31)$$

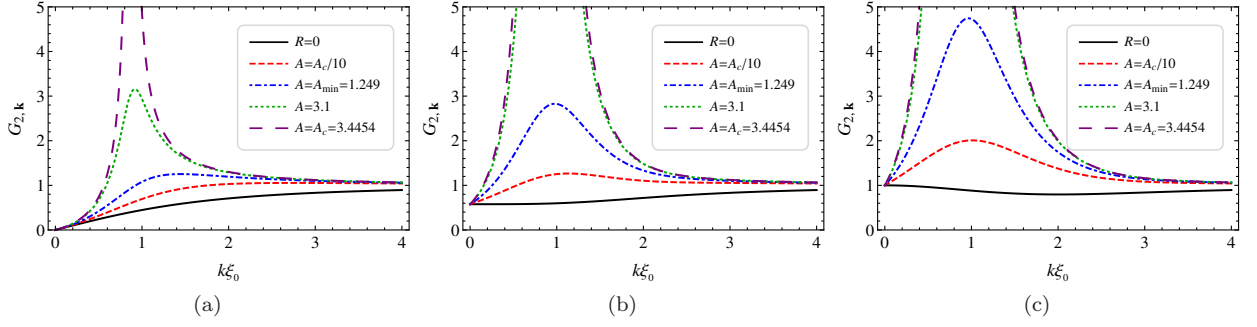


FIG. 2. (Color online) *Stationary state density-density correlations for increasing temperature (from left to right).* The density-density correlation function $G_{2,\mathbf{k}}$ in thermal and quasiparticle ground states. The initial temperatures are (a) $T/mc_0^2 = 0$, (b) $T/mc_0^2 = 1/\sqrt{3}$, and (c) $T/mc_0^2 = 1$. The black solid line corresponds to contact interaction, $R = 0$ ($A = A_c/10$). DDI dominated cases ($R = \sqrt{\pi/2}$) are shown by the remaining curves with A specified in the insets.

For the contact interaction, i.e., $R = 0$ case, we reproduce the result of Ref. [14]. On the other hand, we see that for finite relative strength R and density of dipoles encapsulated in A , both R and A enter the correlation function. For $k \rightarrow 0$, $G_{2,\mathbf{k}}$ simply approaches the dimensionless temperature T/mc_0^2 ; one can thus determine the temperature of the gas by examining the low-momentum density fluctuations.

When $\omega_{\mathbf{k}}/T \gg 1$, we have $\coth(\omega_{\mathbf{k}}/2T) \simeq 1$, so that Eq. (30) becomes

$$G_{2,\mathbf{k}} \simeq \frac{k\xi_0/2}{\sqrt{\left(\frac{k\xi_0}{2}\right)^2 + 1 - \frac{3R}{2}k\xi_0\sqrt{Aw}\left[\frac{k\xi_0}{\sqrt{2}}\sqrt{A}\right]}}. \quad (32)$$

Again, the difference to the contact case $R = 0$ is manifest, because the relative strength and density of dipoles are explicitly involved via R and A , respectively. In the high-momentum limit of free particles $k\xi_0 \gg 1$, $G_{2,\mathbf{k}}$ approaches unity, regardless of temperature and interactions [58].

B. Criteria for nonseparability and steerability of quasiparticle pairs

Pair production in a time-dependent background can be caused by quasiparticles already present, e.g. in a thermal state, or emerge from quasiparticle quantum vacuum fluctuations. The created pairs possess opposite momenta \mathbf{k} and $-\mathbf{k}$ and are correlated. To study their correlations, we restrict ourselves to the consideration of bipartite quantum states.

We focus on quantum correlations represented by entanglement, the notion coined by Schrödinger in 1935 [59], which will here be represented by nonseparable and steerable quasiparticle states. *Steering*, as introduced by Schrödinger in the same year [60], refers to the correla-

tions that can be observed between the outcomes of measurements applied on half of an entangled state (Alice) and the resulting post-measurement states that are then left with the other party (Bob). A criterion testing quantum steering can be seen as an entanglement test where one of the parties (Alice) performs *uncharacterized* measurements, i.e. with a procedure not accessible (hidden in a black box) to the other party (Bob) [61]. Steerable entangled quantum states are a strict subset of nonseparable states, and a strict superset of states exhibiting Bell nonlocality [62–64].

Criteria to assess the degrees of correlation between the created quasiparticles using density-density correlations have previously been analyzed in detail in Refs. [14, 27]. Nonseparability and steerability of quasiparticle pairs are achieved when

$$G_{2,\mathbf{k}}(\tau) < G_{2,\mathbf{k}}^{\text{vac}} = (u_{\mathbf{k}} + v_{\mathbf{k}})^2 \quad [\text{Nonseparable}], \quad (33)$$

and

$$G_{2,\mathbf{k}}(\tau) < \frac{1}{2}G_{2,\mathbf{k}}^{\text{vac}} \quad [\text{Steerable}]. \quad (34)$$

Here, $G_{2,\mathbf{k}}^{\text{vac}}$ is the correlation due to quasiparticle vacuum fluctuations. Whenever $G_{2,\mathbf{k}}(\tau)$ dips below its vacuum value for some times, the state is necessarily nonseparable. Compared with the nonseparability condition in (33), the criterion for steerability shown in (34) is obviously more stringent (as it should be), due to the factor of 1/2 on the right hand side, again reflecting the fact that quasiparticle states exhibiting steering form a subset of nonseparable states. We also note here that a concrete experimental protocol to assess quasiparticle entanglement by the covariance matrix of the quasiparticle quadratures was proposed in Ref. [33].

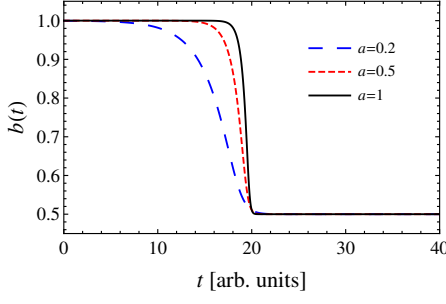


FIG. 3. (Color online) The scale factor $b(t)$ in (36), as a function of the lab time t , showing the compression of the condensate for various speed of sound quench rates a (in arbitrary units of inverse time). Here, we take $c_i^2/c_f^2 = 1/2$.

IV. DYNAMICAL CASIMIR EFFECT

A. Rapid changes of the sound speed

We now impose a time-dependent background by assuming that $c^2 = c^2(\tau)$ is of the form

$$\frac{c^2(\tau)}{c_f^2} = \frac{1}{2} \left(1 + \frac{c_i^2}{c_f^2} \right) + \frac{1}{2} \left(1 - \frac{c_i^2}{c_f^2} \right) \tanh(a\tau). \quad (35)$$

We choose this form of the quench of the sound speed for a direct comparison with the results of [14], and do indeed find that $R = 0$ reproduces the results of the latter reference. The above $c^2(\tau)$, in particular, implies two asymptotic values, $c_i^2 = c_0^2$ and c_f^2 which are obtained when $\tau \rightarrow -\infty$ and $\tau \rightarrow \infty$, respectively, and for which the gas and thus the quasiparticle vacuum become stationary. In the examples below, we quench the system to a larger sound speed $c_f > c_i$.

According to (4) and (19), for constant g_d and g_c , the scale factor is, given a prescribed form of $c^2(\tau)$ as in (35)

$$b(\tau) = \frac{1}{f^2(\tau)} = \frac{c_0^2}{c^2(\tau)}. \quad (36)$$

The gas, for $c_f > c_i$, therefore contracts, with $b(t_f) < b(t_i)$. We plot the scale factor $b(t)$ with respect to the lab time t in Fig. 3, for various quench rates a of the speed of sound in (35).

As a consequence of the temporal change of c^2 , the quasiparticle state is probed by the operators $\hat{\varphi}_{\pm\mathbf{k}}(\tau)$ whose equation of motion is Eq. (17). From the time dependence of the excitation frequencies $\omega_{\mathbf{k}}(\tau)$, the Bogoliubov coefficients $\alpha_{\mathbf{k}}(\tau)$ and $\beta_{\mathbf{k}}(\tau)$ are functions of scaling time τ as well, satisfying the evolution equations (25). The corresponding correlation function in the first line

of Eq. (29) becomes

$$G_{2,\mathbf{k}}(\tau) = (u_{\mathbf{k}}(\tau) + v_{\mathbf{k}}(\tau))^2 [|\alpha_{\mathbf{k}}(\tau)|^2 + |\beta_{\mathbf{k}}(\tau)|^2 + 2\Re\{\alpha_{\mathbf{k}}(\tau)\beta_{\mathbf{k}}^*(\tau)e^{-2i\omega_{\mathbf{k}}\tau'}\}] (2n_{\mathbf{k}}^{\text{in}} + 1). \quad (37)$$

We can rewrite Eq. (37) in the form of Eq. (29), with

$$2n_{\mathbf{k}} + 1 = (|\alpha_{\mathbf{k}}|^2 + |\beta_{\mathbf{k}}|^2)(2n_{\mathbf{k}}^{\text{in}} + 1), \quad c_{\mathbf{k}} = \alpha_{\mathbf{k}}\beta_{\mathbf{k}}^*(2n_{\mathbf{k}}^{\text{in}} + 1). \quad (38)$$

For adiabatic variations ($a \rightarrow 0$ in (35)), $\alpha_{\mathbf{k}}$ and $\beta_{\mathbf{k}}$ do essentially not change and remain very close to 1 and 0, respectively; $G_{2,\mathbf{k}}$ then varies in time only because $(u_{\mathbf{k}} + v_{\mathbf{k}})^2$ does so. However, when we are in a nonadiabatic regime, $\alpha_{\mathbf{k}}$ and $\beta_{\mathbf{k}}$ evolve in time, and the degree of nonadiabaticity is encoded in them. We conclude from Eq. (38) that initial thermal quasiparticle noise can enhance quasiparticle production because the quantities shown in (38), which occur in (29), are proportional to the initial thermal background multiplicative factor $2n_{\mathbf{k}}^{\text{in}} + 1$. However, let us note that while the quasiparticle production is enhanced as regards their sheer number, this happens at the expense of entanglement, since the thermally stimulated pairs are not quantum mechanically correlated.

With the time evolution of $c^2(\tau)$ as prescribed in Eq. (35), we obtain the time-dependent $\omega_{\mathbf{k}}(\tau)$ in (18), and then can solve the coupled Eqs. (25) numerically. In Fig. 4 we show some examples of the evolution of the quasiparticle frequencies at fixed momentum (left panel), and the corresponding correlation function response in Eq. (37) to this evolution (right panel). In what follows, we will use the following definitions of healing length and effective chemical potential, respectively:

$$\xi_f = \frac{1}{mc_f}, \quad \tilde{A} = \frac{mc_f^2}{\omega_{z,0}} = A \frac{c_f^2}{c_i^2}. \quad (39)$$

Note that $\omega_{z,0}$ is constant in the comoving frame. Hence $\tilde{A}/A = c_f^2/c_i^2$ depends on the initial and final speeds of sound only.

The quasiparticle frequencies approach two asymptotics because $c^2(\tau)$ approaches constants in the limits of $\tau \rightarrow -\infty$ and $\tau \rightarrow \infty$, respectively (left panel of Fig. 4). For $k\xi_f = 1$, when $\tilde{A} < 1.073$, the initial frequencies $\omega_{\mathbf{k}i} = \lim_{\tau \rightarrow -\infty} \omega_{\mathbf{k}}(\tau)$ are smaller than the final frequencies $\omega_{\mathbf{k}f} = \lim_{\tau \rightarrow \infty} \omega_{\mathbf{k}}(\tau)$. However, when \tilde{A} is large (assuming DDI dominance, $R = \sqrt{\pi/2}$), i.e., $1.073 < \tilde{A} \leq 3.4454$ for $k\xi_f = 1$, the initial frequencies $\omega_{\mathbf{k}i} = \lim_{\tau \rightarrow -\infty} \omega_{\mathbf{k}}(\tau)$ are larger than the corresponding final ones, $\omega_{\mathbf{k}f} = \lim_{\tau \rightarrow \infty} \omega_{\mathbf{k}}(\tau)$. Therefore (a dominant) DDI, together with a sufficiently high (but experimentally feasible, cf. the discussion in [42]) density of

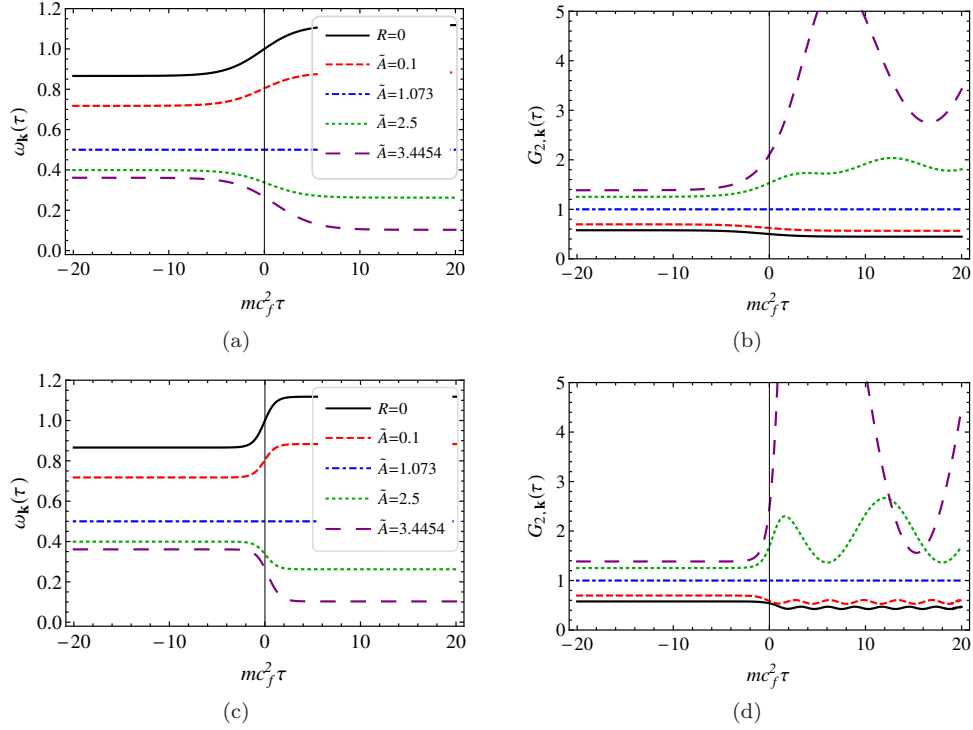


FIG. 4. (Color online) *Time-dependence of Bogoliubov excitation frequencies and density-density correlations.* The Bogoliubov excitation energy $\omega_{\mathbf{k}}$ (plots (a) and (c)) and the corresponding correlation function in Eq. (37) (plots (b) and (d)) for zero temperature as a function of the parametrized time $mc_f^2 \tau$. Here we fix $k\xi_f := 1$, $c_i^2/c_f^2 = 1/2$. The rate of change in (35) is taken as $a/\omega_{\mathbf{k}i} = 0.3$ for plots (a) and (b), and $a/\omega_{\mathbf{k}i} = 1$ for plots (c) and (d). The black solid curves correspond to contact interaction, $R = 0$ ($\tilde{A} = 0.1$). The DDI dominated case ($R = \sqrt{\pi/2}$) with varying values of \tilde{A} , specified in the insets of (a) and (c), is represented by the other curves.

the gas, which are parametrized by R and \tilde{A} , respectively, can significantly affect the quasiparticle response when comparing with a gas possessing only contact interactions. In the presence of a (sufficiently strong) DDI, a roton minimum appears. For increasing roton depth, finite-momentum excitation frequencies near the roton minimum are small; hence these modes are more sensitive to temporal changes of the background.

In the two asymptotical regimes, one has a well defined vacuum for the quasiparticles. These vacua are not necessarily equivalent to each other. The vacuum defined in the far-past region are seen as a two-mode squeezed state from the viewpoint of the observer in the far-future region. That is to say, although there are no quasiparticles at the beginning, due to an expansion or contraction of the condensate, excitations will be created from the quasiparticle vacuum.

The temporal behavior of the correlation function in Eq. (37) is strongly affected by the strength of the DDI and the gas density (see right panel of Fig. 4). When the variation in time of $\omega_{\mathbf{k}}$ is slow, i.e., when a is small, $G_{2,\mathbf{k}}(\tau)$ varies smoothly for small \tilde{A} ($\tilde{A} < 1.073$ in Fig. 4). When the change of c^2 is sufficiently abrupt, the two-

point density correlation function oscillates such that it can periodically dip below its vacuum value. For large \tilde{A} ($\tilde{A} > 1.073$ in Fig. 4), the corresponding two-point density correlations oscillate with larger amplitude than for smaller \tilde{A} (smaller chemical potential).

It is interesting to note that when $k\xi_f = 1$ and $\tilde{A} \approx 1.073$ and with DDI dominating (i.e., $R = \sqrt{\pi/2}$), the frequency of quasiparticles is time-independent. The reason is that in this case the interaction energy, $\mathcal{A}_{\mathbf{k}}$, shown in Eq. (13) is equal to zero, and thus the frequency given in Eq. (18) is reduced to the single-particle part $\mathcal{H}_{\mathbf{k}}$, which is time-independent. This, then, implies that there are no quasiparticles created by the quench. We thus find that the corresponding density-density correlations are time-independent as well.

B. Quench production of nonseparability and steerability

In an experiment, a measurement is performed on the condensate at some given time τ_m . To study quantum correlations between the produced quasiparticle modes, we focus here on the variation of the correlation function

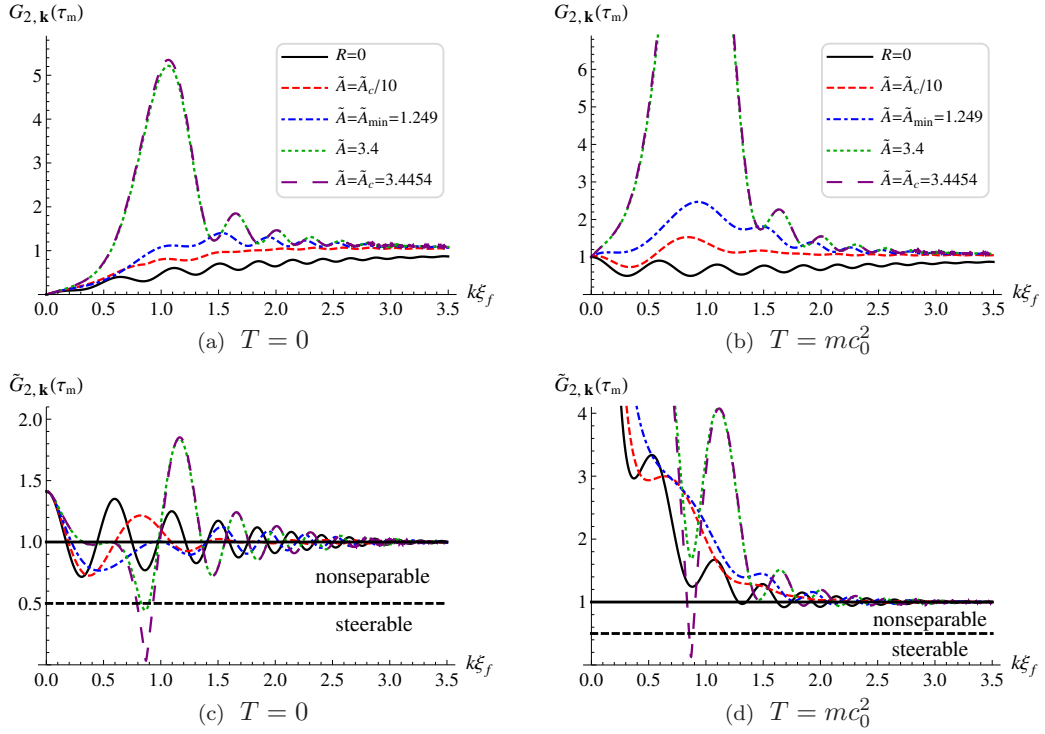


FIG. 5. (Color online) *Density-density correlations as a function of $k\xi_f$ at zero temperature (left) and finite temperature (right).* The measurement time is $\tau_m = 5 \times (mc_f^2)^{-1}$. Here $c_i^2/c_f^2 = 1/2$, and the rate of change $a/\omega_{\mathbf{k}i} = 1$ ($k\xi_f = 3$). The solid curve corresponds to contact interaction, $R = 0$ ($\tilde{A} = \tilde{A}_c/10$). DDI dominance ($R = \sqrt{\pi/2}$) for the other curves, with \tilde{A} specified in the insets of (a) and (b). The lower plots show correlation functions normalized by $(u_{\mathbf{k}} + v_{\mathbf{k}})^2$, such that the nonseparability and steerability thresholds occur at 1 (thick black line) and 1/2 (dashed thick black line), respectively.

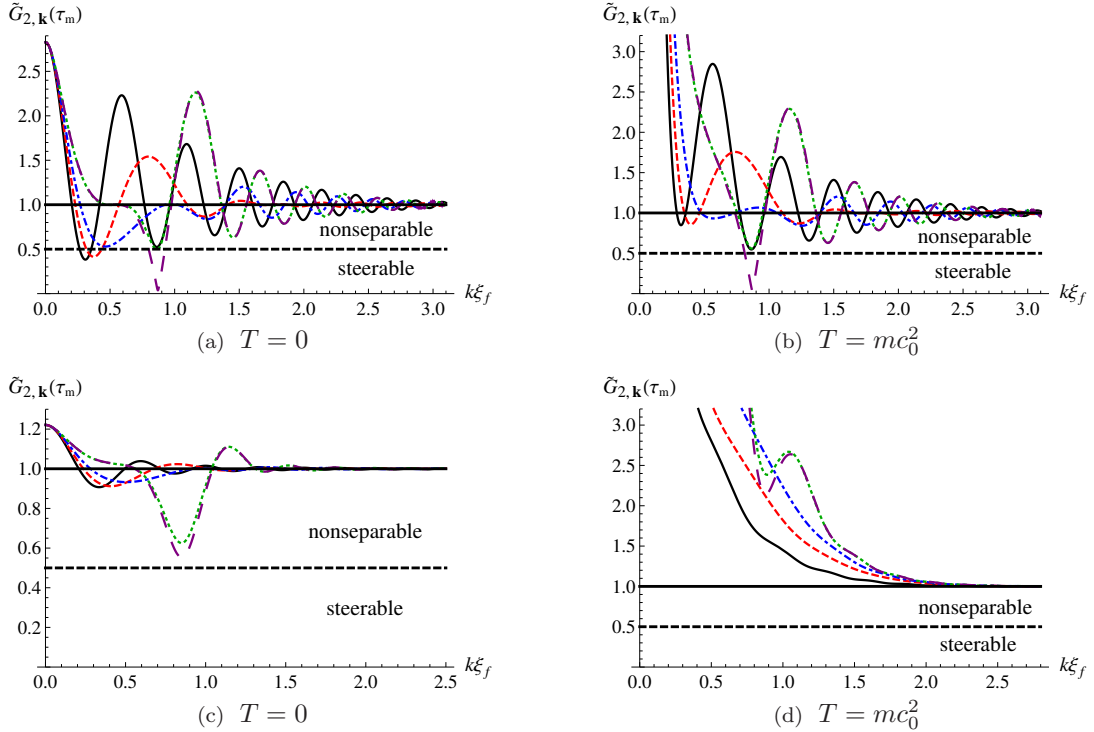


FIG. 6. (Color online) *Varying c_f^2 and sweep rate a for zero temperature (left) and finite temperature (right).* Shown is the variation of the normalized density-density correlation functions with $k\xi_f$ at fixed measurement time $\tau_m = 5 \times (mc_f^2)^{-1}$. (a) and (b) Larger final sound speed $c_i^2/c_f^2 = 1/8$ than in Fig. 5 (a) and (b), with identical rate of change $a/\omega_{\mathbf{k}i} = 1$ ($k\xi_f = 3$). (c) and (d) Smaller sweep rate than in Fig. 5 (c) and (d), with identical $c_i^2/c_f^2 = 1/2$, and the rate of change $a/\omega_{\mathbf{k}i} = 0.05$ ($k\xi_f = 3$). The values of \tilde{A} corresponding to the various curves are found in the insets of Fig. 5 (a) and (b).

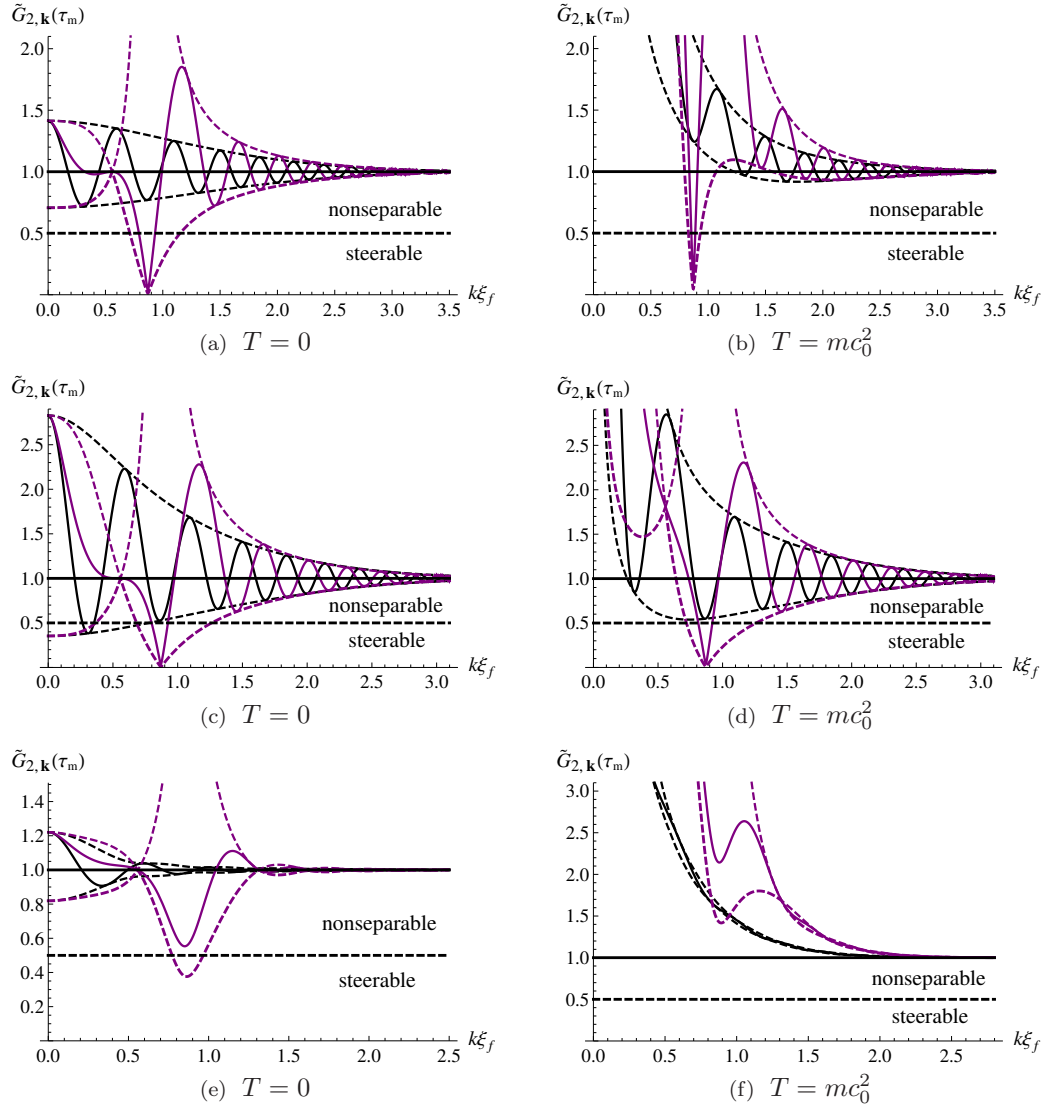


FIG. 7. (Color online) *Density-density correlations as a function of $k\xi_f$ at zero temperature (left) and finite temperature (right).* The measurement time is $\tau_m = 5 \times (mc_f^2)^{-1}$. Here $c_i^2/c_f^2 = 1/2$, and the rate of change $a/\omega_{\mathbf{k}i} = 1$ ($k\xi_f = 3$) for (a) and (b); $c_i^2/c_f^2 = 1/8$, and the rate of change $a/\omega_{\mathbf{k}i} = 1$ ($k\xi_f = 3$) for (c) and (d). Finally, $c_i^2/c_f^2 = 1/2$, and the rate of change $a/\omega_{\mathbf{k}i} = 0.05$ ($k\xi_f = 3$) for (e) and (f). The black solid curves corresponds to contact interaction, $R = 0$ ($\tilde{A} = \tilde{A}_c/10$). The solid purple curves are for the DDI-dominated case ($R = \sqrt{\pi/2}$) at criticality, $\tilde{A} = 3.4454$. The dashed lines are envelopes. Correlation functions are normalized by $(u_{\mathbf{k}} + v_{\mathbf{k}})^2$, such that the nonseparability and steerability thresholds occur at 1 (thick black line) and $1/2$ (dashed thick black line), respectively.

with momentum $k\xi_f$ at fixed time τ_m . As an example, we plot in Fig. 5 the variation of the correlation function in the momentum at fixed measurement time $\tau = \tau_m$. To examine nonseparability and steerability between the produced quasiparticles, we plot the normalized correlation function, i.e. the correlation function divided by its vacuum value

$$\tilde{G}_{2,\mathbf{k}}(\tau) := \frac{G_{2,\mathbf{k}}}{G_{2,\mathbf{k}}^{\text{vac}}} = \frac{G_{2,\mathbf{k}}}{(u_{\mathbf{k}} + v_{\mathbf{k}})^2}. \quad (40)$$

The nonseparability and steerability thresholds then occur according to Eqs. (33) and (34) at $\tilde{G}_{2,\mathbf{k}} = 1$ and $\tilde{G}_{2,\mathbf{k}} = 1/2$, respectively.

The normalized density-density correlation function periodically changes and potentially dips below unity. When the normalized density-density correlation function is smaller than 1 for some times, the final quasiparticle state is nonseparable. This implies that entanglement is created between quasiparticles with opposite momenta \mathbf{k} and $-\mathbf{k}$ due to the nonadiabatic variation of the speed of sound of the condensate and the excitation of the con-

densate vacuum. Moreover, even though initial thermal noise decreases the range of nonseparable \mathbf{k} 's (right panel of Fig. 5), a sufficiently dense dipolar gas close to criticality still creates entanglement (comparing (d) with (c) in Fig. 5). In particular, looking at Fig. 5(d), the momentum which renders the final quasiparticle state nonseparable, that is which satisfies the inequality (33), is for the dipolar gas smaller than for a contact interaction gas.

Although the sufficient condition (34) for steerability might not be satisfied for any value of \mathbf{k} in the final quasiparticle state when only contact interactions are present, a sufficiently large DDI rather generically induces a state which does satisfy this criterion for some momenta (see the green dotted and purple long-dashed curves in (c) of Fig. 5). As discussed in subsection III B, steerability is a more stringent correlation property of quantum states than nonseparability is (however, still weaker than Bell nonlocality). Steering implies that the state is nonseparable but not vice versa, a fact which is readily confirmed with Figs. 5 and 6.

The time-dependent speed of sound as specified in (35) can, for example, be adjusted by the external potential trapping the condensate, according to the scaling equations (3) and (4). To determine how the quench rate and final sound speed squared, c_f^2 , affect the creation of quasiparticle entanglement, we plot the normalized density-density correlation functions in Fig. 6. We conclude that quantum steering between quasiparticles is robustly obtained whenever we are near criticality $\tilde{A} \lesssim \tilde{A}_c$. In addition, we observe that an increase of c_f^2 amplifies the fluctuations of the normalized density-density correlation functions around their mean values (comparing (a) in Fig. 6 with (c) in Fig. 5), and induces the creation of quasiparticle steering in a condensate with relatively low density ($\tilde{A} < \tilde{A}_{\min}$). On the other hand, smaller sweep rates $a/\omega_{\mathbf{k}i}$ decrease the amplitude of the fluctuations of the normalized density-density correlation functions (comparing (c) in Fig. 6 with (c) in Fig. 5); they also decrease the production of quasiparticle steering near criticality, especially for the thermal case (more details are revealed from inspecting the envelopes in Fig. 7).

After the quench, the final spectrum $\omega_{\mathbf{k}}$ of quasiparticles becomes time-independent, and the factor $e^{-2i \int^\tau \omega_{\mathbf{k}}(\tau') d\tau'}$ in Eq. (37) is then simply $e^{-2i\omega_{\mathbf{k}}\tau}$. The density-density correlation function (37) or its normalized version (40) then periodically oscillates. We therefore can verify whether the final quasiparticles are entangled by looking at the corresponding envelopes, i.e., by determining the maximum and minimum values reached by the density-density correlation function (40) as it oscillates in time. With the criteria for nonseparability and

steerability displayed in (33) and (34), respectively, the quasiparticles are entangled or even steerable when the lower envelope for the normalized correlations dips below 1 and 1/2, respectively.

To show the domains of nonseparability and steerability more clearly, and make the comparison between the contact interaction case and the DDI case more readily accessible, in Fig. 7 we plot the envelopes for the contact interaction case and the DDI case with the critical value of $\tilde{A} = 3.4454$ shown in Figs. 5 and 6. We conclude that, when DDI dominates, the created quasiparticles with wave vectors near the roton minimum satisfy the sufficient criterion (34) for steerability, while this is not the case for contact interactions. Therefore, we conclude that compared to a gas with solely repulsive contact interactions, the DDI Bose gas system displays an enhanced potential for the presence of steering in the bipartite quantum state of quasiparticle pairs resulting from the quench. This enhancement is generally robust against thermal noise, and variation of the difference between the initial and final speeds of sound as well as of the quench rate.

One notices from Fig. 7 that there is an exceptional point where the upper and the lower envelopes cross. At this point, the normalized density-density correlation functions are equal to unity in the zero temperature limit. This requires that the Bogoliubov coefficient $\beta_{\mathbf{k}}(\tau)$ vanishes, implying that for these momenta there are no quasiparticles created. This, in turn, is due to the fact that the interaction energy $\mathcal{A}_{\mathbf{k}}(\tau)$ in (18) equals zero, and thus the spectrum is time-independent. Vanishing $\mathcal{A}_{\mathbf{k}}(\tau)$ is due to the fact that the Fourier transform of the interaction $V_{\text{int},0}^{2D}(k)$ in (13) crosses zero for a certain momentum when $R > \frac{2}{3}\sqrt{\pi/2}$ (i.e., when $g_{d,0} > g_{c,0}$ [42]). The phenomenon just described does not happen for contact interactions, where the Fourier transform is simply a constant, so that $\beta_{\mathbf{k}}$ is non-zero for all momenta.

Let us, finally, note from Fig. 7 that the maxima of the upper envelopes at the roton minimum are very large, and that the momentum range for the lower envelopes to satisfy the steerability criterion is relatively narrow. Hence, care in choosing the appropriate measurement time τ_m and appropriate momentum \mathbf{k} needs to be exercised, to reliably judge whether in a given experiment the created quasiparticles satisfy the entanglement criteria.

V. CONCLUSION

We have studied the production of quasiparticle pairs in a quasi-two-dimensional dipolar condensate undergoing a rapid temporal variation of its speed of sound, and

focused on criteria using the experimentally accessible density-density correlation function [24], to determine the nonseparability and steerability of the final quasiparticle state. As demonstrated in Figs. 5, 6 and 7, the DDI between the gas particles significantly enhances the potential for the creation of entanglement (nonseparability and steering), being established between quasiparticle modes \mathbf{k} and $-\mathbf{k}$. We conclude that the dipolar two-body interaction leads to increased quantum correlations, as encoded in the bipartite continuous-variable

state of quasiparticles created by a quench.

ACKNOWLEDGMENTS

ZT and SYC were supported by the BK21 Plus Program (21A2013111123) funded by the Ministry of Education (MOE, Korea) and National Research Foundation of Korea (NRF). SYC and URF were supported by the NRF, Grant No. 2017R1A2A2A05001422.

-
- [1] N. D. Birrell and P. C. W. Davies, “Quantum Fields in Curved Space,” (Cambridge University Press, Cambridge, England, 1982).
 - [2] Erwin Schrödinger, “The proper vibrations of the expanding universe,” *Physica* **6**, 899–912 (1939).
 - [3] L. Parker, “Particle Creation in Expanding Universes,” *Phys. Rev. Lett.* **21**, 562–564 (1968).
 - [4] Gerald T. Moore, “Quantum Theory of the Electromagnetic Field in a Variable-Length One-Dimensional Cavity,” *Journal of Mathematical Physics* **11**, 2679–2691 (1970).
 - [5] S. W. Hawking, “Particle creation by black holes,” *Communications in Mathematical Physics* **43**, 199–220 (1975).
 - [6] M. Visser, “Hawking Radiation without Black Hole Entropy,” *Phys. Rev. Lett.* **80**, 3436–3439 (1998).
 - [7] Nature Physics Insight, “Quantum simulation,” *Nat. Phys.* **8** (April 2012).
 - [8] W. G. Unruh, “Experimental Black-Hole Evaporation?” *Phys. Rev. Lett.* **46**, 1351–1353 (1981).
 - [9] Uwe R. Fischer and Matt Visser, “On the space-time curvature experienced by quasiparticle excitations in the Painlevé–Gullstrand effective geometry,” *Annals of Physics* **304**, 22–39 (2003).
 - [10] C. Barceló, S. Liberati, and M. Visser, “Analogue Gravity,” *Living Reviews in Relativity* **14** (2011), 10.12942/lrr-2011-3.
 - [11] P. O. Fedichev and U. R. Fischer, ““Cosmological” quasiparticle production in harmonically trapped superfluid gases,” *Phys. Rev. A* **69**, 033602 (2004).
 - [12] Ralf Schützhold, Michael Uhlmann, Lutz Petersen, Hector Schmitz, Axel Friedenauer, and Tobias Schätz, “Analogue of Cosmological Particle Creation in an Ion Trap,” *Phys. Rev. Lett.* **99**, 201301 (2007).
 - [13] I. Carusotto, R. Balbinot, A. Fabbri, and A. Recati, “Density correlations and analog dynamical Casimir emission of Bogoliubov phonons in modulated atomic Bose-Einstein condensates,” *The European Physical Journal D* **56**, 391–404 (2010).
 - [14] Scott Robertson, Florent Michel, and Renaud Parentani, “Controlling and observing nonseparability of phonons created in time-dependent 1D atomic Bose condensates,” *Phys. Rev. D* **95**, 065020 (2017).
 - [15] J. R. Johansson, G. Johansson, C. M. Wilson, and Franco Nori, “Dynamical Casimir Effect in a Superconducting Coplanar Waveguide,” *Phys. Rev. Lett.* **103**, 147003 (2009).
 - [16] Zehua Tian, Jiliang Jing, and Andrzej Dragan, “Analog cosmological particle generation in a superconducting circuit,” *Phys. Rev. D* **95**, 125003 (2017).
 - [17] C. M. Wilson, G. Johansson, A. Pourkabirian, M. Simoen, J. R. Johansson, T. Duty, F. Nori, and P. Delsing, “Observation of the dynamical Casimir effect in a superconducting circuit,” *Nature* **479**, 376–379 (2011).
 - [18] Pasi Lähteenmäki, G. S. Paraoanu, Juha Hassel, and Pertti J. Hakonen, “Dynamical Casimir effect in a Josephson metamaterial,” *Proceedings of the National Academy of Sciences* **110**, 4234–4238 (2013).
 - [19] J.-C. Jaskula, G. B. Partridge, M. Bonneau, R. Lopes, J. Ruauadel, D. Boiron, and C. I. Westbrook, “Acoustic Analog to the Dynamical Casimir Effect in a Bose-Einstein Condensate,” *Phys. Rev. Lett.* **109**, 220401 (2012).
 - [20] C.-L. Hung, V. Gurarie, and C. Chin, “From Cosmology to Cold Atoms: Observation of Sakharov Oscillations in a Quenched Atomic Superfluid,” *Science* **341**, 1213–1215 (2013).
 - [21] M. Visser, “Acoustic black holes: horizons, ergospheres and Hawking radiation,” *Classical and Quantum Gravity* **15**, 1767 (1998).
 - [22] U. R. Fischer and R. Schützhold, “Quantum simulation of cosmic inflation in two-component Bose-Einstein condensates,” *Phys. Rev. A* **70**, 063615 (2004).
 - [23] Roberto Balbinot, Alessandro Fabbri, Serena Fagnocchi, Alessio Recati, and Iacopo Carusotto, “Nonlocal density correlations as a signature of Hawking radiation from acoustic black holes,” *Phys. Rev. A* **78**, 021603 (2008).
 - [24] Jeff Steinhauer, “Measuring the entanglement of analogue Hawking radiation by the density-density correlation function,” *Phys. Rev. D* **92**, 024043 (2015).
 - [25] P. D. Nation, M. P. Blencowe, A. J. Rimberg, and E. Buks, “Analogue Hawking Radiation in a dc-SQUID Array Transmission Line,” *Phys. Rev. Lett.* **103**, 087004 (2009).
 - [26] J. R. M. de Nova, F. Sols, and I. Zapata, “Entanglement and violation of classical inequalities in the Hawking radiation of flowing atom condensates,” *New Journal of Physics* **17**, 105003 (2015).
 - [27] Scott Robertson, Florent Michel, and Renaud Parentani, “Assessing degrees of entanglement of phonon states in atomic Bose gases through the measurement of commuting observables,” *Phys. Rev. D* **96**, 045012 (2017).

- [28] H. S. Nguyen, D. Gerace, I. Carusotto, D. Sanvitto, E. Galopin, A. Lemaître, I. Sagnes, J. Bloch, and A. Amo, “Acoustic Black Hole in a Stationary Hydrodynamic Flow of Microcavity Polaritons,” *Phys. Rev. Lett.* **114**, 036402 (2015).
- [29] Oren Lahav, Amir Itah, Alex Blumkin, Carmit Gordon, Shahar Rinott, Alona Zayats, and Jeff Steinhauer, “Realization of a Sonic Black Hole Analog in a Bose-Einstein Condensate,” *Phys. Rev. Lett.* **105**, 240401 (2010).
- [30] Jeff Steinhauer, “Observation of self-amplifying Hawking radiation in an analogue black-hole laser,” *Nat. Phys.* **10**, 864–869 (2014).
- [31] Jeff Steinhauer, “Observation of quantum Hawking radiation and its entanglement in an analogue black hole,” *Nat. Phys.* **12**, 959–965 (2016).
- [32] S. Eckel, A. Kumar, T. Jacobson, I. B. Spielman, and G. K. Campbell, “A Rapidly Expanding Bose-Einstein Condensate: An Expanding Universe in the Lab,” *Phys. Rev. X* **8**, 021021 (2018).
- [33] Stefano Finazzi and Iacopo Carusotto, “Entangled phonons in atomic Bose-Einstein condensates,” *Phys. Rev. A* **90**, 033607 (2014).
- [34] M. A. Baranov, “Theoretical progress in many-body physics with ultracold dipolar gases,” *Physics Reports* **464**, 71–111 (2008).
- [35] Thierry Lahaye, Tobias Koch, Bernd Fröhlich, Marco Fattori, Jonas Metz, Axel Griesmaier, Stefano Giovanazzi, and Tilman Pfau, “Strong dipolar effects in a quantum ferrofluid,” *Nature* **448**, 672–675 (2007).
- [36] Mingwu Lu, Nathaniel Q. Burdick, Seo Ho Youn, and Benjamin L. Lev, “Strongly Dipolar Bose-Einstein Condensate of Dysprosium,” *Phys. Rev. Lett.* **107**, 190401 (2011).
- [37] K. Aikawa, A. Frisch, M. Mark, S. Baier, A. Rietzler, R. Grimm, and F. Ferlaino, “Bose-Einstein Condensation of Erbium,” *Phys. Rev. Lett.* **108**, 210401 (2012).
- [38] Goulven Quémener and Paul S. Julienne, “Ultracold Molecules under Control!” *Chemical Reviews* **112**, 4949–5011 (2012).
- [39] Mingyang Guo, Bing Zhu, Bo Lu, Xin Ye, Fudong Wang, Romain Vexiau, Nadia Bouloufa-Maafa, Goulven Quémener, Olivier Dulieu, and Dajun Wang, “Creation of an ultracold gas of ground-state dipolar $^{23}\text{Na}^{87}\text{Rb}$ molecules,” *Phys. Rev. Lett.* **116**, 205303 (2016).
- [40] Timur M. Rvachov, Hyungmok Son, Ariel T. Sommer, Sepehr Ebadi, Juliana J. Park, Martin W. Zwierlein, Wolfgang Ketterle, and Alan O. Jamison, “Long-lived ultracold molecules with electric and magnetic dipole moments,” *Phys. Rev. Lett.* **119**, 143001 (2017).
- [41] L. Santos, G. V. Shlyapnikov, and M. Lewenstein, “Roton-Maxon Spectrum and Stability of Trapped Dipolar Bose-Einstein Condensates,” *Phys. Rev. Lett.* **90**, 250403 (2003).
- [42] Uwe R. Fischer, “Stability of quasi-two-dimensional Bose-Einstein condensates with dominant dipole-dipole interactions,” *Phys. Rev. A* **73**, 031602 (2006).
- [43] Shai Ronen, Daniele C. E. Bortolotti, and John L. Bohn, “Radial and Angular Rotons in Trapped Dipolar Gases,” *Phys. Rev. Lett.* **98**, 030406 (2007).
- [44] Stefan S. Natu, L. Campanello, and S. Das Sarma, “Dynamics of correlations in a quasi-two-dimensional dipolar Bose gas following a quantum quench,” *Phys. Rev. A* **90**, 043617 (2014).
- [45] Seok-Yeong Chä and Uwe R. Fischer, “Probing the Scale Invariance of the Inflationary Power Spectrum in Expanding Quasi-Two-Dimensional Dipolar Condensates,” *Phys. Rev. Lett.* **118**, 130404 (2017).
- [46] L. Landau, “On the Theory of Superfluidity,” *Phys. Rev.* **75**, 884–885 (1949).
- [47] F. Mezei, “High-Resolution Study of Excitations in Superfluid ^4He by the Neutron Spin-Echo Technique,” *Phys. Rev. Lett.* **44**, 1601–1604 (1980).
- [48] Holger Kadau, Matthias Schmitt, Matthias Wenzel, Clarissa Wink, Thomas Maier, Igor Ferrier-Barbut, and Tilman Pfau, “Observing the Rosensweig instability of a quantum ferrofluid,” *Nature* **530**, 194–197 (2016).
- [49] Igor Ferrier-Barbut, Holger Kadau, Matthias Schmitt, Matthias Wenzel, and Tilman Pfau, “Observation of Quantum Droplets in a Strongly Dipolar Bose Gas,” *Phys. Rev. Lett.* **116**, 215301 (2016).
- [50] L. Chomaz, R. M. W. van Bijnen, D. Petter, G. Faraoni, S. Baier, J. H. Becher, M. J. Mark, F. Wächtler, L. Santos, and F. Ferlaino, “Observation of roton mode population in a dipolar quantum gas,” *Nature Physics* **14**, 442–446 (2018).
- [51] Matthias Wenzel, Fabian Böttcher, Tim Langen, Igor Ferrier-Barbut, and Tilman Pfau, “Striped states in a many-body system of tilted dipoles,” *Phys. Rev. A* **96**, 053630 (2017).
- [52] Yu. Kagan, E. L. Surkov, and G. V. Shlyapnikov, “Evolution of a Bose-condensed gas under variations of the confining potential,” *Phys. Rev. A* **54**, R1753–R1756 (1996).
- [53] Y. Castin and R. Dum, “Bose-Einstein Condensates in Time Dependent Traps,” *Phys. Rev. Lett.* **77**, 5315–5319 (1996).
- [54] Vladimir Gritsev, Peter Barmettler, and Eugene Demler, “Scaling approach to quantum non-equilibrium dynamics of many-body systems,” *New Journal of Physics* **12**, 113005 (2010).
- [55] Y. Castin, “Bose-Einstein Condensates in Atomic Gases: Simple Theoretical Results,” in *Coherent atomic matter waves*, Les Houches Session LXXII, edited by R. Kaiser, C. Westbrook, and F. David (Springer, Berlin, 2001) pp. 1–136.
- [56] Xavier Busch, Renaud Parentani, and Scott Robertson, “Quantum entanglement due to a modulated dynamical Casimir effect,” *Phys. Rev. A* **89**, 063606 (2014).
- [57] Chen-Lung Hung, Xibo Zhang, Li-Chung Ha, Shih-Kuang Tung, Nathan Gemelke, and Cheng Chin, “Extracting density-density correlations from in situ images of atomic quantum gases,” *New Journal of Physics* **13**, 075019 (2011).
- [58] The function $\zeta w[\zeta]$ occurring in $G_{2,k}$ approaches a constant in this limit [42].
- [59] E. Schrödinger, “Die gegenwärtige Situation in der Quantenmechanik,” *Naturwissenschaften* **23**, 823–828 (1935).
- [60] E. Schrödinger, “Discussion of Probability Relations between Separated Systems,” *Mathematical Proceedings of the Cambridge Philosophical Society* **3**, 447–451 (1935).
- [61] D Cavalcanti and P Skrzypczyk, “Quantum steering: a review with focus on semidefinite programming,” *Reports on Progress in Physics* **80**, 024001 (2017).
- [62] H. M. Wiseman, S. J. Jones, and A. C. Doherty, “Steering, Entanglement, Nonlocality, and the Einstein-Podolsky-Rosen Paradox,” *Phys. Rev. Lett.* **98**, 140402 (2007).

- [63] S. J. Jones, H. M. Wiseman, and A. C. Doherty, “Entanglement, Einstein-Podolsky-Rosen correlations, Bell non-locality, and steering,” *Phys. Rev. A* **76**, 052116 (2007).
- [64] M. D. Reid, “Demonstration of the Einstein-Podolsky-Rosen paradox using nondegenerate parametric amplification,” *Phys. Rev. A* **40**, 913–923 (1989).